



# Study on energy distribution of reflected particles from plasma facing materials

Y. Hasegawa <sup>a,\*</sup>, S. Masuzaki <sup>b</sup>, N. Noda <sup>b</sup>, N. Ohyabu <sup>b</sup>, A. Sagara <sup>b</sup>,  
H. Suzuki <sup>b</sup>, A. Komori <sup>b</sup>, T. Morisaki <sup>b</sup>, O. Motojima <sup>b</sup>, V.S. Voitsenya <sup>c</sup>

<sup>a</sup> *Department of Fusion Science, School of Mathematical and Physical Science, The Graduate University for Advanced Studies, 322-6, Oroshi, Toki 509-5292, Japan*

<sup>b</sup> *National Institute for Fusion Science, Oroshi, Toki 509-52, Japan*

<sup>c</sup> *Institute for Plasma Physics, National Science Center, Kharkov Institute of Physics and Technology, 310108 Kharkov, Ukraine*

---

## Abstract

Reflection of ions at a tungsten target was investigated experimentally in a linear plasma device. The tungsten target plate was set perpendicular to the magnetic field, and irradiated by hydrogen and helium plasma. The experiment measures a current as a function of sheath potential for a fixed angle. The reflected neutral particles from the target plate are measured by neutral-negative charge converter made of Cu. The experimental results show good agreement with the results calculated with TRIM Monte-Carlo simulation code. A possibility to estimate the ion temperature is shown through the sheath potential dependence of the ion reflection in the low energy range. © 1999 Elsevier Science B.V. All rights reserved.

*Keywords:* Ion reflection; Ion temperature; TRIM simulation; TPD-I

---

## 1. Introduction

Ion reflection is one of the particle recycling processes in fusion devices. Some of ions striking the plasma facing surface are backscattered with a large fraction of the incident ion energy. Usually the energy of the reflected particles is much higher than that of the particles emitted by desorption from a surface and those dissociated by Frank-Condon processes. Thus it is necessary to take a contribution of the ion reflection into account to study the recycling, the energy balance, heat load on the divertor plate or limiter and core plasma performances. The ion reflection has been studied numerically by computer simulations and experimentally using ion beam devices. Recently, measurement of the energy distribution of the reflected particles was performed with an ion beam incidence [1]. This result has shown a good agreement with the calculated result by TRIM code [2].

The data of the ion reflection, such as energy or angular distribution of the reflected particles under the plasma condition including the effects of the magnetic field and finite ion temperature have been not studied systematically.

The aim of this work is to study systematically the energy distribution of the reflected particles from the plasma facing surfaces. The energy distribution of the reflected particles is affected by the experimental condition, such as components of plasma ions, plasma facing materials, the angle between the material surface and magnetic field line, potential drop between the plasma and material surface. Almost all the reflected particles are neutral in the energy range of the edge plasma [3]. To measure the reflected neutral particles, a neutral-negative charged particle converter is used. This method is suitable because of its good sensitivity to low energy particles (>20 eV) [4]. In this paper, a comparison between experimental results of steady state reflected particles and calculation results based on TRIM.SP. code is given. The expected energy distribution of the reflected particles is discussed.

---

\* Corresponding author. Tel.: +81-572 58 2222/1221; fax: +81-572 58 2618; e-mail: hasegawa@rouge.nifs.ac.jp

## 2. Experimental setup

The experiment has been carried out in the linear plasma device TPD-I [5]. Steady state hydrogen and helium plasmas are produced by arc discharge under the condition of magnetic field  $B \sim 0.2$  T. Fig. 1 shows the schematic drawing of the experimental setup TPD-I. The target plate is made of tungsten with a size of  $10 \times 10$  mm and produced by hot press. Before plasma irradiation, the target surface was treated by electrolysis polishing. After series experiments, target surface is analyzed by SEM and EDX. From this results, the impurity is not observed on the target surface. The back side of the target plate is coated with ceramic to avoid a diffusion flow from the back side. The target plate is set perpendicular to the magnetic field line. A 1 mm  $\phi$  tungsten wire, covered by ceramic tube, supports the target plate. The ceramic tube plays a role of the electric isolator from plasma current. Electron density, temperature and space potential were measured by a fast scanning Langmuir probe located 20 mm away from the target plate. In the present series of experiments, the range of electron density and temperature are  $3.2 < n_e < 5.5 \times 10^{17} \text{ m}^{-3}$  and  $6.4 < kT_e < 14.4$  eV for hydrogen discharge,  $1.1 < n_e < 2.3 \times 10^{18} \text{ m}^{-3}$  and  $1.9 < kT_e < 8.5$  eV for helium discharge in present experiment, respectively. In TPD-I plasmas, the incident ion energy is dominated by the potential drop of electrostatic sheath in front of the target plate. Impact energy distribution is detected by ion temperature and sheath potential. The

bias voltage gives the change of incident ion energy. The sheath potential is determined from bias voltage and space potential which measures the fast scanning Langmuir probe. The pressure in discharge was measured with a diaphragm gauge.

The detector system for the reflected particles is set with an angle of 65 degree to the magnetic field on TPD-I. It consists of a fixed slit, flight tube and detector chamber. The distance between target plate and the fixed slit is 567 mm. The slit size is  $6.6 \times 0.2$  mm. The detector chamber has a separate pumping system and is differentially pumped with this slit. The pressure in the flight tube is kept in the order of  $10^{-4}$  Pa. The distance between target plate to detector chamber is  $\sim 2.6$  m to avoid influence of the magnetic field in the detector chamber. The solid angle between target plate and neutral-negative convertor in the detector chamber is always fixed. The solid angle is defined by two slits. The size of target plate ( $10 \times 10$  mm) is smaller than length between target plate and slit near the gate valve (567 mm). The solid angle is  $4.1 \times 10^{-6} \text{ sr}$  ( $= 6.6 \times 0.2/567^2$ ). The reflected particles went through the flight tube and struck the neutral-negative convertor made of Cu. Negative particles means not only electron but negative ion. We introduce express 'negative particle' in accordance with reference [6]. Negative particle emission coefficient of the Cu plate by neutral particles ( $\gamma^-$ ) is an important parameter to evaluate the energy distribution. We have used the values reported by Verbeek for H and by Hayden for He. An analytical equation has been

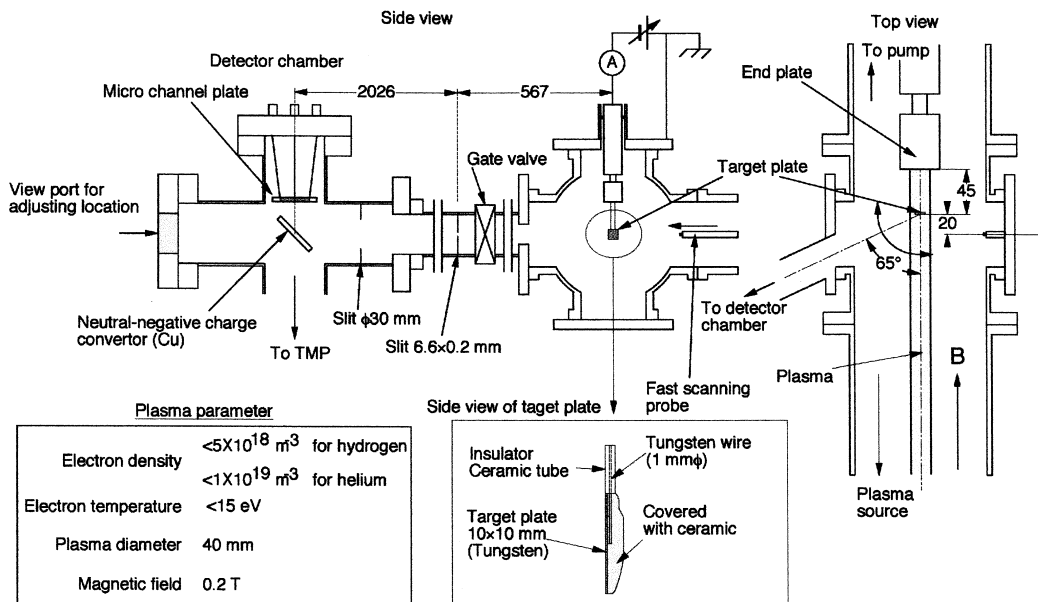


Fig. 1. Experimental setup for measurement of the reflected particles from the tungsten target plate in TPD-I. In this figure, the magnetic coils is hidden.

obtained for the relation between  $\gamma^-$  and impact neutral energy in the range from 10 to 1000 eV. This relation has been utilized for the calculation as following [6,7]:

$$Y = \sum_{k=1}^n a_k X^k, \quad (1)$$

where  $Y = \log \gamma^-$  and  $X = \log E$ ,  $E$  is the incident energy with a unit in eV. The  $a_k$  values are shown in Table 1. The fitting error increases in the course of lower energies. The negative charged particles emitted from the Cu plate are collected by a electron multiplier (+500 V) which is a micro channel plate (MCP) with a gain  $G_{\text{MCP}} = 10^4$  at 1000 V. The electron current from the MCP is converted to voltage by a loading resistor (10 k $\Omega$ ), amplified with voltage gain ( $G_{\text{PA}} = 10^5$ ). The output signal  $V_{\text{out}}$  shows below:

$$V_{\text{out}}(E_s) = \int_0^{\infty} \gamma^-(E) \eta(E) \frac{dN}{dE d\Omega} dE \frac{\Omega}{4\pi} G_{\text{MCP}} G_{\text{PA}} I_{\text{sat}}, \quad (2)$$

where  $dN/dE d\Omega$  [eV sr] is distribution of the energy distribution,  $I_{\text{sat}}$  is ion saturate current to the target plate,  $E_s$  is sheath potential in front of target plate and  $\eta(E)$  is the product of the fraction  $\xi(E)$  of the reflected neutrals not scattered by the background gas and the efficiency  $\varepsilon$  of electron collection by the MCP. The fraction  $\xi(E)$  is depend on the energy of the reflected particles, and  $\varepsilon$  is a constant.

### 3. Calculation

The Monte-Carlo simulation code TRIM.SP. (version TRVMC) is utilized for calculation of the reflected particles flux [8]. The parameters needed for calculation are assumed as follow; the Krypton-Carbon potential as the screened Coulomb potential between incident and target atoms, the local and continuous electronic energy losses as Oen–Robinson model and Lindhard–Scharff model, respectively, and a planner surface potential assumption with a binding energy of 1 eV for chemical binding force is used. The density of tungsten was given as 19.29 g/cm<sup>3</sup>.

The direction of the incident angle of the magnetic field is assumed to be normal to the target plate. There

Table 1

The coefficient for the  $g(E)$  in Eq. (1)

	H	He
$a_0$	$-5.62 \times 10^0$	$-2.31 \times 10^1$
$a_1$	$4.51 \times 10^0$	$2.76 \times 10^1$
$a_2$	$-1.30 \times 10^0$	$-1.34 \times 10^1$
$a_3$	$1.45 \times 10^{-1}$	$3.16 \times 10^0$
$a_4$		$-2.99 \times 10^{-1}$

are three regions in the model as follows; (1) the plasma region (hydrogen and helium plasma), (2) the sheath region and (3) the target plate (tungsten target). The energy distribution of ions is assumed to be isotropic three-dimensional Maxwellian in plasma region. In the sheath region, ions are accelerated by the sheath potential, and assumed to be collisionless. The target plate surface is considered to be flat and pure. The incident ion flux from the plasma to the sheath region can be expressed as below:

$$\Gamma(T_i) = \frac{1}{2\pi} \left( \frac{m}{kT_i} \right)^2 \int_{-\infty}^{\infty} dv_x \int_{-\infty}^{\infty} dv_y \int_0^{\infty} dv_z v_z \exp \left\{ - \frac{m_i(v_x^2 + v_y^2 + v_z^2)}{2kT_i} \right\}, \quad (3)$$

where  $k$  is the Boltzmann's constant,  $m_i$  is the ion mass,  $x$  and  $y$  is the parallel direction to target surface,  $z$  is the perpendicular direction to target surface. The azimuthal symmetry is assumed for the reflected particles. The normalized flux to the sheath region is below:

$$d\Gamma(E, \theta, T_i) = \frac{E}{(kT_i)^2} \sin 2\theta \exp \left\{ - \frac{E}{kT_i} \right\} dE d\theta, \quad (4)$$

where  $E$  is the kinetic energy of particles,  $v_{\perp} (= (v_x^2 + v_y^2)^{1/2})$  and  $v_{\parallel} (= v_z)$  is the parallel and perpendicular velocity, respectively.  $E = m_i(v_{\perp}^2 + v_{\parallel}^2)/2$ , and  $\theta$  is the pitch angle in plasma region. In the sheath region, the energy distribution is shifted Maxwellian due to the acceleration by the sheath potential  $q\Phi_s$  in which  $q$  is ion charge and  $\Phi_s$  is sheath potential. Pre-sheath potential is included. The incident ion energy  $E_t$  to the target can be obtained by  $E + q\Phi_s$ . The incident angle  $\Theta$  of ions to the target in this region can be obtained using the pitch angle  $\theta$ , ion kinetic energy  $E$  and sheath potential  $q\Phi_s$  as below:

$$\tan \Theta = \frac{\sqrt{E} \sin \theta}{\sqrt{E \cos^2 \theta + q\Phi_s}}. \quad (5)$$

The incident ion flux to the target can be obtained as below;

$$d\Gamma(E_t, \theta, T_i, \Phi_s) = \left\{ \frac{E_t - q\Phi_s}{(kT_i)^2} \sin 2\theta \exp \left\{ - \frac{E_t - q\Phi_s}{kT_i} \right\} dE d\theta (E_t \geq q\Phi_s) 0 (E_t < q\Phi_s) \right\}. \quad (6)$$

The incident angle and the energy flux of ions to the target are given by Eqs. (5) and (6), respectively. A large sheath potential reduces incident angle of the particles.

4. Result and discussion

To evaluate the reflected particles, normalized value  $P_{Cu-e}$  is introduced. This value is probability of the negative charge release when incident particles go into the target plate. Two  $P_{Cu-e}$  values are defined as follows:

$$P_{Cu-e}^{TRIM} = \int_0^\infty \gamma(E)\eta(E) \frac{dN}{dE d\Omega} dE, \tag{7}$$

$$P_{Cu-e}^{EXP.} = \frac{V_{out}(E_s)}{G_{MCP} G_{PA} I_{sat} \frac{\Omega}{4\pi}}, \tag{8}$$

$P_{Cu-e}^{TRIM}$  is calculated through Eq. (7) with the incident flux from Eq. (6) and incident angle from Eq. (5). From Eq. (8),  $P_{Cu-e}^{EXP.}$  is estimated from experimental data of  $V_{out}(E)$  and  $I_{sat}$ . Fig. 2 shows a dependence of  $P_{Cu-e}^{EXP.}$  on the sheath potential for various working gas pressure. From this pressure dependence, scattering cross section

with neutral gas is obtained in this geometry. The scattering cross section  $\sigma_{sc}$  is defined below:

$$P_{Cu-e}^{EXP.}(P) \propto \exp \left\{ -\frac{L_\Pi}{L_{MFP}} \right\},$$

$$L_{MFP} = \frac{1}{n_0 \sigma_{sc}}, \tag{9}$$

where  $L_\Pi$  and  $L_{MFP}$  is the flight length and the mean free path in the characteristic pressure,  $n_0$  is the neutral particle density. It is found that through calculation that the reflected particle energy distribution has a peak near the incident energy with low impact energy.  $\sigma_{sc}$  is a function of the reflected particles energy. The  $\sigma_{sc}$  values are in the order of  $10^{-16}$  cm<sup>2</sup> [9]. The average scattering cross section changes in factor 2 between 50 and 150 eV [9]. If  $\zeta(E)$  is constant,  $P_{Cu-e}^{EXP.}$  values are underestimation in the low energy region. The energy dependence of  $\gamma^-(E)$  changes some magnitude of order under 150 eV and is larger than  $\zeta(E)$ . We assume that  $\zeta(E)$  is constant with the energy in this energy region in this geometry at first approximation.  $P_{Cu-e}^{EXP.}$  depends on only  $\gamma^-(E)$  from Eq. (7). Experimental and calculation data have a good agreement when  $\eta=0.20$  is given at 1.0 mTorr for hydrogen discharge and  $\eta=0.21$  at 0.9 mTorr for helium discharge for  $T_i=1$  eV. This means that the reflected energy distribution derived from the calculation agrees well with that in the experiment. From the calculation, energy spectrum of the reflected particles ( $= dN/dE d\Omega$ ) does not change significantly at low energy region. However the  $P_{Cu-e}^{EXP.}$  value is changed. When the incident energy distribution has a finite ion temperature, spread of incident energy distribution is recognized from  $E_s$  to

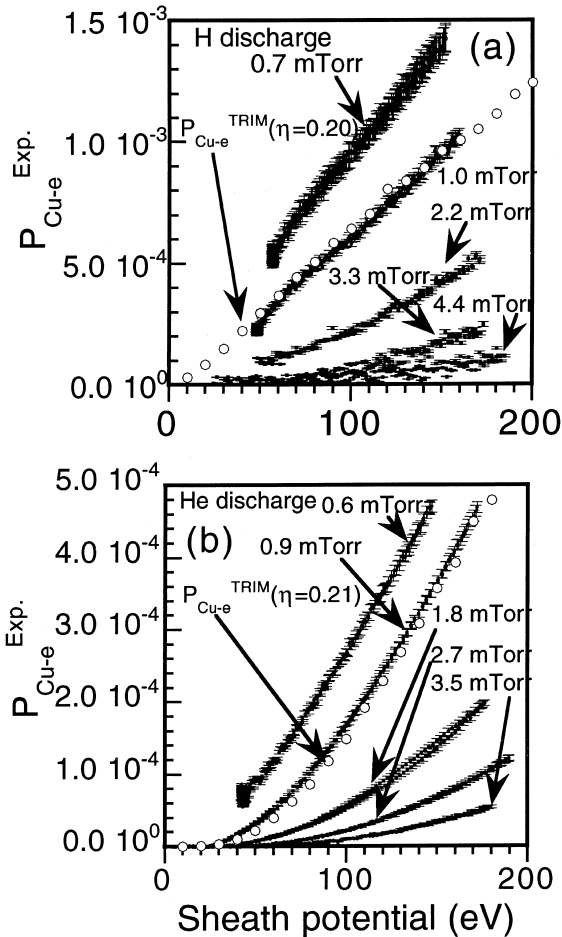


Fig. 2. The dependence of the sheath potential in various pressure (a) hydrogen and (b) helium discharge case.

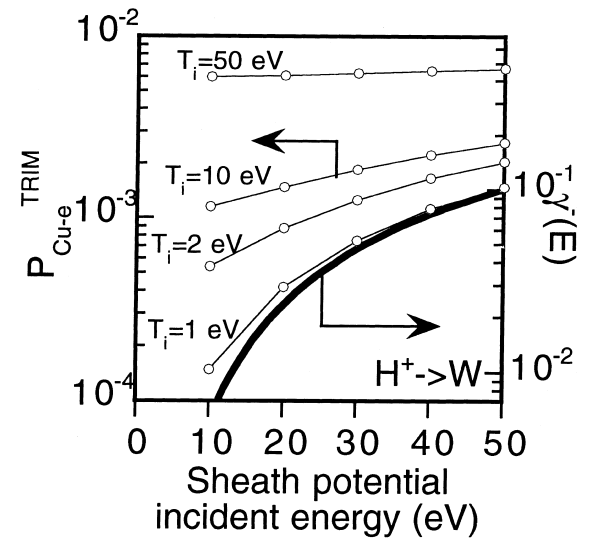


Fig. 3. Calculation results  $P_{Cu-e}^{TRIM}$  to estimate the ion temperature by using the reflected particles from the tungsten target plate.

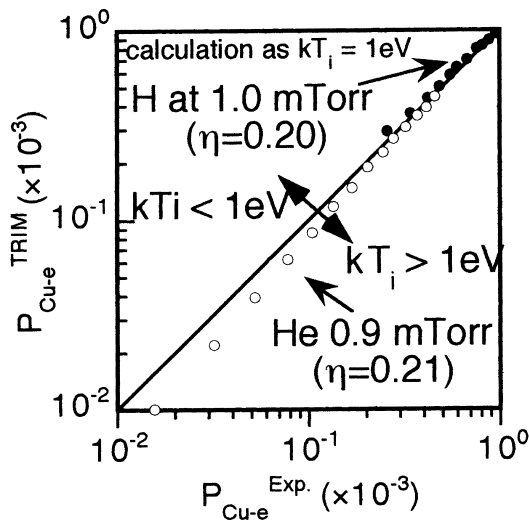


Fig. 4. The relation between  $P_{\text{Cu-e}}^{\text{Exp}}$  and  $P_{\text{Cu-e}}^{\text{TRIM}}$  to assume  $T_i = 1$  eV.

about  $E_s + 6kT_i$ . This energy is affected to impact energy distribution of the reflected particles. Spread in energy spectrum of the reflected particles gives affected to  $P_{\text{Cu-e}}^{\text{Exp}}$  in low energy region in Eq. (1). Compared with experimental and calculation data which is assumed some ion temperature by Eq. (6), it is possible to estimate incident energy distribution to the target plate in the low energy region. Fig. 3 shows  $P_{\text{Cu-e}}^{\text{TRIM}}$  for various  $kT_i$  and  $\gamma^-(E)$  for hydrogen in same dynamics range.  $P_{\text{Cu-e}}^{\text{TRIM}}$  increases with increasing  $kT_i$ . When  $kT_i$  is below 10 eV, ion temperature is estimated from this results. From obtained the

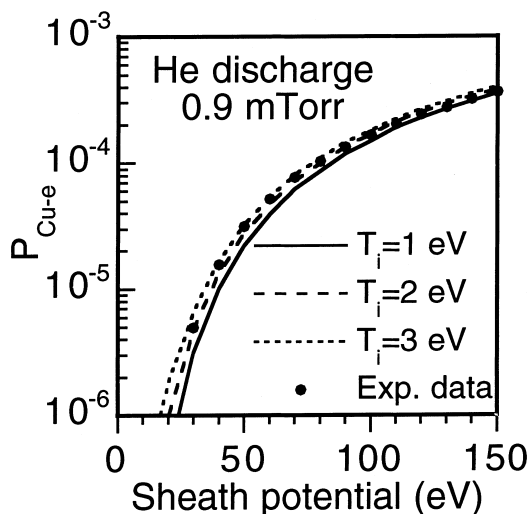


Fig. 5. Estimation of ion temperature for helium discharge from the various  $kT_i$  case.

$P_{\text{Cu-e}}^{\text{Exp}}$  and  $P_{\text{Cu-e}}^{\text{TRIM}}$ , ion temperature is estimated in TPD-I. Fig. 4 shows the relation between experimental and calculated results including  $\eta$  above mention with assumption  $kT_i = 1$  eV case. In the case of the hydrogen, ion temperature is estimated under 1 eV. The hydrogen data of  $P_{\text{Cu-e}}^{\text{Exp}}$  does not exist under the 40 eV in Fig. 2(a) due to deep floating potential. However in the case of helium discharge, ion temperature is estimated over 1 eV. Fig. 5 shows the relation between sheath potential and  $P_{\text{Cu-e}}$  in various  $kT_i$ . This results suggest that ion temperature is between 2 and 3 eV with helium discharge at 0.9 mTorr in TPD-I.

## 5. Summary

The reflected neutral particles were measured in the linear device TPD-I. Experimental data were compared with calculated ones obtained by simulation code including the effects of the finite ion temperature and sheath potential in front of the target material. The pressure dependence of the reflected particles is related to the scattering cross section in this geometry and mean free path. There is a good agreement between experimental and calculated results taking account of scattering with neutral gas and collecting efficiency of the negative charge. From this feature, there is a possibility to estimate the ion temperature using by the sheath potential dependence of the  $P_{\text{Cu-e}}^{\text{Exp}}$  value with an assumption of energy distribution of the reflected particles from the calculation. Finally, ion temperatures are under 1 eV at 1.0 mTorr for hydrogen discharge and 2–3 eV at 0.9 mTorr for helium discharge.

For understanding the ion reflection, we plan to measure the reflected energy distribution with the Time-of-Flight technique in order to obtain more precise energy distribution of the reflected particles.

## Acknowledgements

Authors would like to thank Dr W. Eckstein and IPP-Garching for providing TRIM.SP. code and valuable discussions. Authors thanks to Takamura laboratory in Nagoya University for their technical supports to fast scanning probe measurement.

## References

- [1] R. Aratari, W. Eckstein, Nucl. Instr. and Meth. B 42 (1989) 11.
- [2] W. Eckstein, Computer simulation of ion-solid interaction, Springer Series in Material Science, vol. 10, Springer, Berlin, 1991.
- [3] R.S. Bhattacharya et al., Surf. Sci. 93 (1980) 563.

- [4] D.E. Voss, Ph.D. Thesis in Princeton 1980, Low Energy Neutral Atom Emission Recycling in the PLT tokamak.
- [5] N. Ezumi et al., *J. Nucl. Mater.* 241–243 (1997) 349.
- [6] H. Verbeek, W. Eckstein, IPP 9/45 (1983).
- [7] H.C. Hayden, N.G. Utterback, *Phys. Rev. A* 135 (6) (1964) 1575.
- [8] Y. Hasegawa et al., New diagnostic method of ion energy distribution in edge plasma, *J. Plasma Fusion Res.*, to be published.
- [9] D.N. Ruzic, PhD thesis in Princeton 1984, Total scattering cross-section and interatomic potentials for neutral hydrogen and helium on some noble gases.